Int J Adv Manuf Technol (2010) 50:13–19
DOI 10.1007/s00170-009-2502-0

ORIGINAL ARTICLE

Rapid casting of turbine blades with abnormal film cooling holes using integral ceramic casting molds

Haihua Wu · Dichen Li · Xiaojie Chen · Bo Sun · Dongyang Xu

Received: 24 April 2009 / Accepted: 18 December 2009 / Published online: 14 January 2010

Abstract Film cooling is an important cooling method to decrease the turbine blade surface temperature, and its average cooling efficiency is mainly dependent on the cooling structures of internal passageways and the shapes of film cooling holes. Compared with standard cylindrical film cooling holes, abnormal film cooling holes have higher average cooling efficiency. But it is difficult to manufacture these holes using traditional machining methods. In this paper, a novel process was developed to fabricate turbine blades with abnormal film cooling holes by combining stereolithography (SL) technology with gelcasting technology. To decrease the drying shrinkage, the freeze-drying technique was applied to treat the wet ceramic casting mold green body surrounded by the SL mold, and the proper sintering process parameters were determined for lowering the sintered shrinkage. Finally, the integral ceramic casting mold was obtained, and a turbine blade with converging–diverging film cooling holes was rapidly cast to verify the feasibility of the proposed process.

Keywords Rapid casting · Turbine blade · Integral ceramic casting mold · Stereolithography · Gelcasting

1 Introduction

With the increase of the inlet temperature of gas turbine, some compulsory cooling measures must be taken to lower the surface temperature of turbine blades and avoid deformation. The film cooling technique has won wide applications in the turbine blades, and cooling air is directed through intricate internal cooling passageways and film cooling holes to maintain the surface temperature within an acceptable range. Several researchers have reported that the average cooling efficiency of abnormal film cooling holes (including fan-shaped holes, converging–diverging holes, dustpan-shaped holes, cone-shaped holes, etc.) is much larger than that of standard cylindrical holes under the same air blowing ratio. For example, as the air blowing ratio is 2, the average cooling effectiveness of converging–diverging holes is 5.6 times that of standard cylindrical holes [1–3]. If standard cylindrical holes are substituted by abnormal film cooling holes, a better film cooling effect will be obtained, and more air will flow into gas turbine combustion chamber to increase the combustion efficiency. It is beneficial to improve the inlet temperature of gas turbine and thrust–weight ratio.

A computer-aided design (CAD) model of turbine blade with converging–diverging film cooling holes is shown in Fig. 1a, and the structural diagram of one converging–diverging film cooling hole is shown in Fig. 1b. The cross-section shape of the inlet is ellipse but the cross-section shape of the outlet is rectangle, and the ratio of the inlet's area to the outlet's area is 90%. In conventional investment casting, a fired ceramic core is positioned in an investment shell mold to form an intricate internal cooling passageway, and the cylindrical film cooling holes are manufactured by laser drilling or electrical discharge machining (EDM). But recasting layers and micro-cracks that appeared in laser drilling or EDM have an unfavorable influence on the fatigue lifetime and safe reliability of turbine blades. Because the cross-section shapes of the inlet and the outlet of abnormal film cooling holes are different, it is difficult to fabricate them

H. Wu · D. Li (✉) · X. Chen · B. Sun · D. Xu
State Key Laboratory of Manufacturing Systems Engineering,
Xi'an Jiaotong University,
Xi'an, People's Republic of China
e-mail: dcli@mail.xjtu.edu.cn

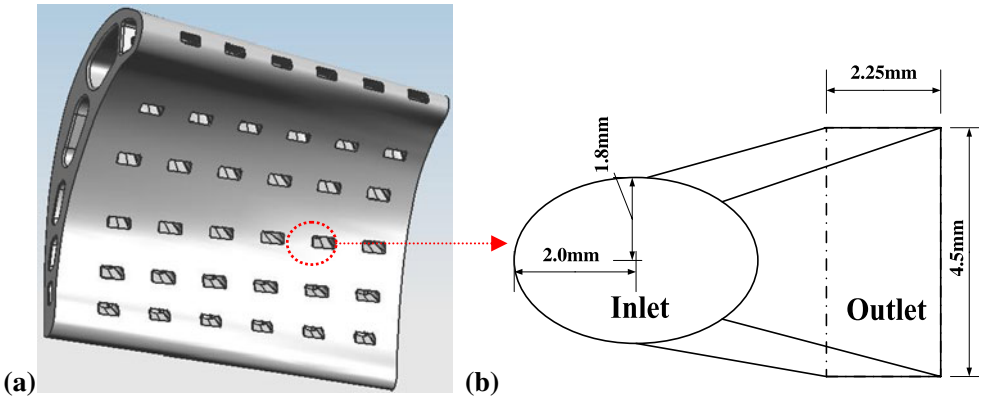

Fig. 1 **a** A turbine blade CAD model with converging–diverging film cooling holes. **b** The structural diagram of one hole (local amplification)

using laser drilling or EDM. This poses a severe challenge to conventional investment casting technology.

If an integral ceramic core shown in Fig. 2 is prepared in advance, the converging–diverging film cooling holes will be fabricated directly in investment casting, and laser drilling or EDM can be eliminated, which is helpful to cut down production time and cost. The Russian Institute of Aeronautical Materials has presented a combination technique to produce the integral ceramic core. Firstly, a complicated ceramic core is decomposed into many simple ones. And then these simple ceramic cores are fabricated respectively. Finally, they are assembled together to produce the complicated one. There are two problems to solve: the first is how to conduct accurate location for all simple ceramic cores and the second is how to reduce high costs and long lead time associated with many metal mold developments.

With the development of rapid prototype (RP) technology, some new processes have been developed to solve the problems mentioned above, such as patternless casting manufacturing, direct shell production casting, generic rapid prototyping systems, and ZCast metal casting. They are utilized to directly produce integral ceramic casting molds (including ceramic cores), where all ceramic cores and shell are naturally connected with each other and the position accuracies between ceramic cores and that between ceramic cores and shell can be ensured. However, the forming efficiency is low and the forming accuracy is poor, and these processes have not been widely applied in industry [4–7]. A silica casting mold has been made from photoactivated ceramic suspensions by utilizing SLA250, but the surface finish quality of aluminum casting produced with such mold is poor [8].

Stereolithography (SL) is one of the most popular RP processes used for rapid tooling applications; it has advantages of high forming accuracy, good rigidity, and well surface quality, and is quite suitable to fabricate molds or models with complex geometry [9]. To short mold development cycle, SL prototypes have been used as metal molds in the low pressure injection molding process [10]. In traditional investment casting, thermally expendable wax patterns can be substituted by the stereolithography-apparatus-built epoxy resin patterns, which will shorten the fabricating time of wax patterns and cost less [11, 12].

Gelcasting, following the development of slip casting and injection molding, is an advanced near-net-shape forming process, and it has been successfully utilized to produce complex-shaped ceramic components [13]. In the paper, a novel process for rapid casting turbine blade with converging–diverging film cooling holes was presented by combining gelcasting technology with SL technology, which includes the following steps: (1) designing and fabricating an SL mold; (2) pouring ceramic slurry into the SL mold, and obtaining an integral ceramic casting mold via in situ polymerizing, freeze-drying, pyrolyzing, and sintering; (3) filling the integral ceramic casting mold with molten metal; (4) removing the ceramic casting mold, and obtaining a turbine blade casting.

2 Rapid casting turbine blade

2.1 Design and fabrication of SL mold

The SL mold was utilized to form the ceramic casting mold green body; its CAD model shown in Fig. 2 was made up

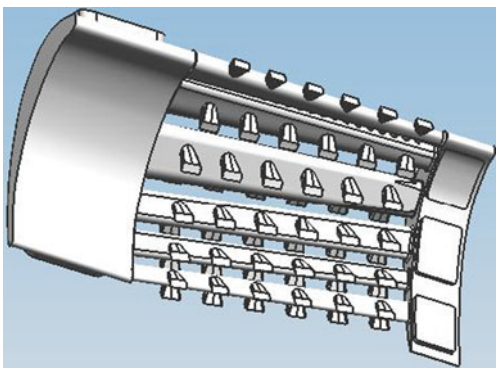

Fig. 2 An integral ceramic core CAD model

of five parts, which were turbine blade prototype 1, resin shell 2, registration portion 3, gating system prototype 4, and voids 5. The turbine blade prototype 1 had an internal cavity corresponding to the desired core configuration and an outer configuration corresponding to the outer geometry desired in the cast product. The resin shell 2 was assembled with the turbine blade prototype 1 to form the SL mold cavity. To eliminate the harmful influence from thick shell on casting metallurgical performance, the distance between them should be controlled in the range from 3 to 8 mm. Voids 5 were filled up by ceramic slurry to form registration portions 3, which connected the turbine blade prototype 1 with the resin shell 2 to maintain correct spatial alignment. The gating system prototype 4 was utilized to produce a ceramic gating system for casting molten metal.

The SL mold made from DSM Somos19120 photosensitive resin was automatically constructed by the apparatus SPS 450B (provided by the Institute of Advanced Manufacturing Technology in Xi'an Jiaotong University of China), and its dimensional tolerance was ±0.05 mm. In the paper, a rapid coating process was applied to eliminate the stair-stepping effects on the SL prototype sloping surface. After coating, surface roughness, R_a, was decreased from 12.5 to 0.4–1.0 μm (Fig. 3).

2.2 Fabrication of integral ceramic casting mold

2.2.1 Preparation of slurry

The high-solid-loading, low-viscosity ceramic slurry was fundamental to fabricate the integral casting mold green body. In order to minimize the drying shrinkage, the solid volume fraction should be improved as high as possible, but the slurry viscosity and filling ability were affected, so the solid volume fraction should be controlled within an acceptable range.

Two types of corundum powders (D_{50}=25 μm and D_{50}= 5 μm, mass fraction=99.32%) supplied by Shandong Zibo Aluminum Inc. China were chosen as matrix materials. Magnesium oxide (D_{50}=2 μm, mass fraction=99.99%) and yttria powders (D_{50}=2 μm, mass fraction=99.99%) provided by Sinopharm Chemical Reagent Co., Ltd. China were used as mineralizers. During sintering, the mineralizers react with finer corundum powders to form high-temperature-resistant polycrystalline compositions (yttrium aluminum garnet and magnesia alumina spinel), which were beneficial to improve the high-temperature properties of the ceramic casting mold [14, 15]. Polyethylene glycol (PEG, average molecular weight of 6,000) was chosen as plasticizer. PEG was an excellent plasticizer with the ability of reducing the drying stress in the wet green body to prevent cracking [16].

A premixed solution with a concentration of 20% was prepared by dissolving acrylamide (monomer, CH_3CONH_2, AM) and *N*,*N*-methylene diacrylamide (cross-linker, $C_7H_{10}N_2O_2$; in 24:1 ratio) in proper amount of deionized water, and then PEG6000 (20 wt.% of AM) and sodium polyacrylate (dispersant, 2.5 wt.% of solid powders) were added. Afterwards, pH value was adjusted to 11 by adding a proper amount of strong ammonia. A mixture, previously prepared of Al_2O_3/Y_2O_3/MgO, was added into the premixed solution in steps. After ball milling for 2–3 h, the ceramic slurry with low viscosity and high solids loading (0.735 Pa·s, 55 vol.%) was obtained.

2.2.2 Gelcasting and freeze drying

After the initiator [ammonium persulfate, $(NH_4)_2S_2O_8$)] and catalyst (*N*,*N*,*N*′,*N*′-tetramethyl ethylenediamine, $C_6H_{16}N_2$; 1 and 0.2 wt.% of the premixed solution, respectively) were added, the ceramic slurry was stirred in vacuum for 3–5 min to eliminate air bubbles. As the ceramic slurry was poured into the SL mold, a vibration (amplitude 1–3 mm, vibration frequency 30–60 Hz) was applied. Subsequently, under the effect of the initiator and catalyst, the ceramic slurry was in situ polymerized to form the ceramic casting mold green body.

The resin shell 2 was removed and the exposed ceramic casting mold green body was put into the FD-0.5 m^2

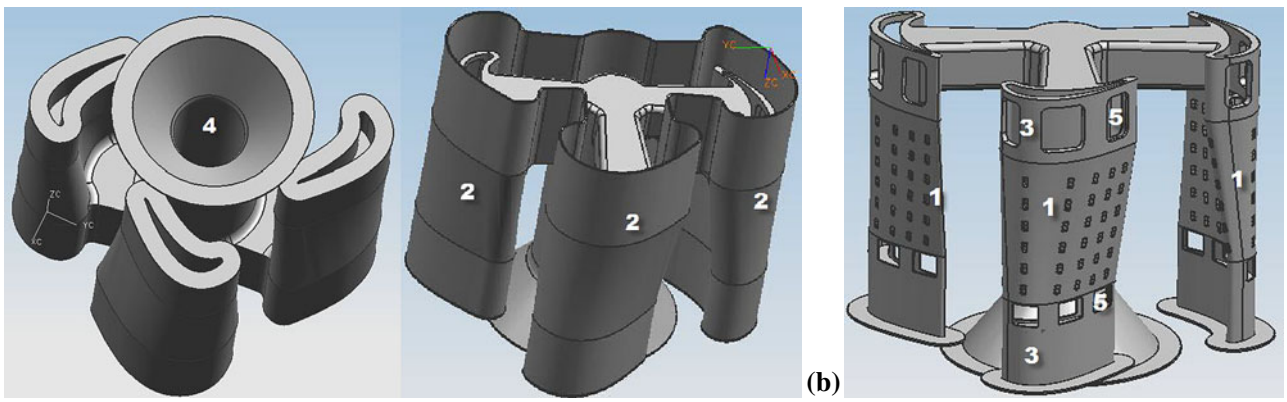

Fig. 3 CAD model of the SL mold: **a** top surface and bottom surface, **b** internal structures

vacuum freeze dryer provided by Zhejiang Sanxiong Machinery Limited Company, China. The green body was first pre-frozen at −30°C for 2–4 h and then sublimed for 24–48 h under a vacuum of 20–30 Pa.

2.2.3 Pyrolyzing and sintering

After freeze drying, the next step was to burn out the binder (i.e., polyacrylamide) and the SL mold prototype. Firstly, the green body was conveyed into the GZL-400/480 high-temperature bell sintering furnace provided by Hefei Risine Heatek Corp., Ltd., China, and heated to 300°C with a heating rate of 20–30°C/h and kept at 300°C for 1 h to burn out the SL mold. Then it was heated to the sintering temperature (1,550°C) at 360–420°C/h heating rate and held for 4–5 h. Finally, it was cooled down to room temperature along with the furnace. After the residual ash of the SL mold was removed by compressed air below 0.2 MPa, the integral ceramic casting mold was obtained.

2.3 Vacuum casting

Vacuum casting was performed in order as follows.

(a) The integral ceramic casting mold was heated to 1,050°C and kept for 1–2 h.
(b) A molten low-alloy structural steel (20CrNiMo) was cast into the ceramic casting mold under a vacuum of 0.613 Pa.
(c) Ceramic shell was removed by mechanical crushing, and ceramic cores were removed with high-temperature alkali solution under alternating pressures.
(d) A turbine blade casting was obtained.

2.4 Performance test

Five specimens (Φ 4 mm×50 mm) were prepared and the average freeze-drying shrinkage was determined by measuring their lengths before and after freeze drying. The lengths of five specimens (Φ 4 mm×50 mm) were measured before and after sintering, and the average sintered shrinkage was calculated. The effect of different material compositions and different sintering process parameters (including sintering temperature, holding time, and heating rate) on the sintered shrinkage was investigated.

3 Results and discussion

An SL prototype and the integral ceramic mold fabricated by the abovementioned process are shown in Fig. 4a and b, respectively. Ceramic cores and shell are connected together via ceramic registration portions (shown in Fig. 4c). In the new process, metal mold is replaced by the complex-shaped SL mold, which can be burnt out, so the demolding step was eliminated, which decreased the possibility of damage of the green body. Compared with the metal molds, the development procedure of the SL mold is easier, and the development cycle is shorter and the cost is lower.

Figure 5 shows defect-free turbine blade castings. It could be seen that all converging–diverging film cooling holes had been cast directly. The surface roughness reached 3.2–6.3 μm, but a higher level was more preferable. According to ISO8062, the dimensional accuracy of the turbine blade castings reached up to CT6–CT7.

Figure 6 shows some defects in the turbine blade castings; some film cooling holes are not formed. The reason was that some corresponding ceramic cores used to form film cooling holes were broken in the fabricating process of the ceramic casting mold. Some technological measures should be taken to maintain the structural integrity of the ceramic casting mold.

The wet green body contained the same amount of water as the starting slurry, and the water should be removed in the drying process; air drying is one of the most common

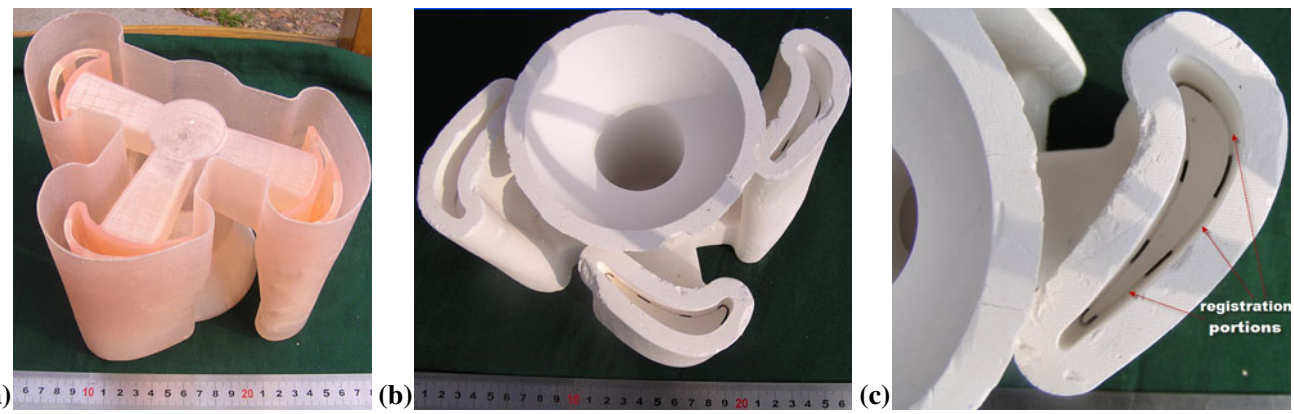

Fig. 4 **a** The SL mold prototype. **b** The integral ceramic mold. **c** The registration portions of cores and shell (local amplification)

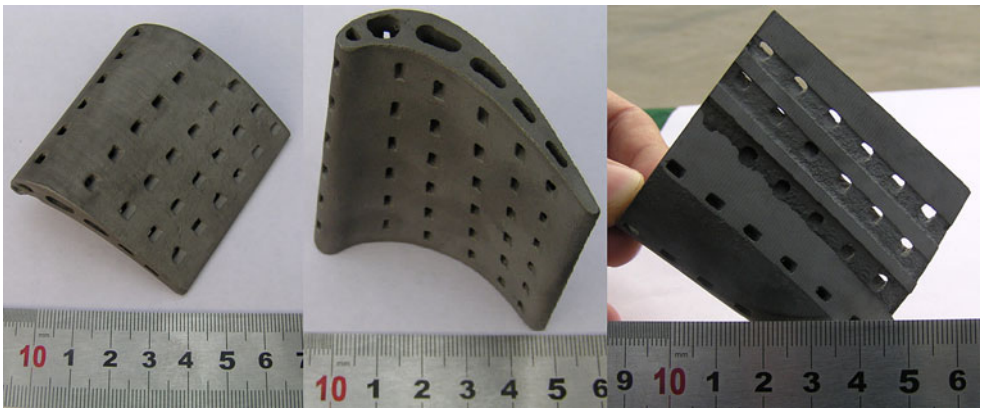

Fig. 5 Defect-free turbine blade castings and one cross section

drying methods. However, the air-drying shrinkage inevitably occurred, which led to the forming of the drying stress. The drying shrinkage was hindered by the SL mold; meanwhile, the wet green body was very weak, and the integral ceramic casting mold was a typical multi-scale component. The ceramic cores used to form the internal cooling passages were thick, but the ceramic cores used to form the film cooling holes were relatively tiny. So cracks might appear on the tiny ceramic cores. In the paper, freeze drying was first introduced to treat with the wet green body to prevent the formation of cracks. For typical 55 vol.% solids loading, the air-drying shrinkage reached about 2.0%, but the freeze-drying shrinkage was only 0.32% as pre-freezing temperature was −30°C, which means that the possibility of cracking was decreased. During freeze drying, the liquid/vapor interfacial energy (the surface tension, i.e., the drying–shrinkage driving force) did not exist, so the apparent shape of the green body could remain unchangeable and the low drying shrinkage was obtained. After ice crystals sublimated, large amounts of interconnected minute pores were left in the green body, which provided the flowing channels for internal water vapor; it is favorable to safely dry out the thick wet green body wrapped by the SL mold.

The binder content in the green body was only ~4 wt.%, so binder removal was neither time consuming nor critical, and the binder could be easily removed by baking. But the epoxy resin was a thermoset material, and its thermal expansion coefficient was one order of magnitude larger than that of the green body. The SL mold prototype did not melt by heating but continued to expand, which led to the thermal stress in the ceramic shell. If the thermal stress exceeded the rupture modulus of the green body, the ceramic shell might crack. Previous research shows that the SL prototype should be designed as the QuickCast build style [17]. In the paper, the turbine blade SL prototype, a porous thin-walled structure part, was safely removed by a slow pyrolyzing process.

Figure 7 shows the sintered shrinkage curve at different sintering temperatures, as the heating rate is 480°C/h and the holding time is 4 h. It can be seen that the sintered shrinkage increased with the sintering temperature. When the sintering temperature reaches 1,600°C, the sintered shrinkage exceeds 1.0%. Excessive sintered shrinkage may result in the slim film cooling cores fracture (see Fig. 8a). At 1,550°C, the sintered shrinkage is about 0.32%, and the slim film cooling cores were intact (see Fig. 8b). The lower sintered shrinkage means higher sintered qualified rate of ceramic cores. Magnesium aluminum spinel ($MgAl_2O_4$, the reaction

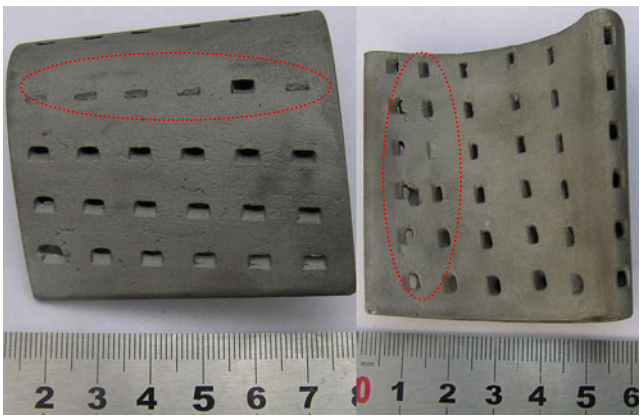

Fig. 6 Turbine blade castings with some film cooling holes unformed

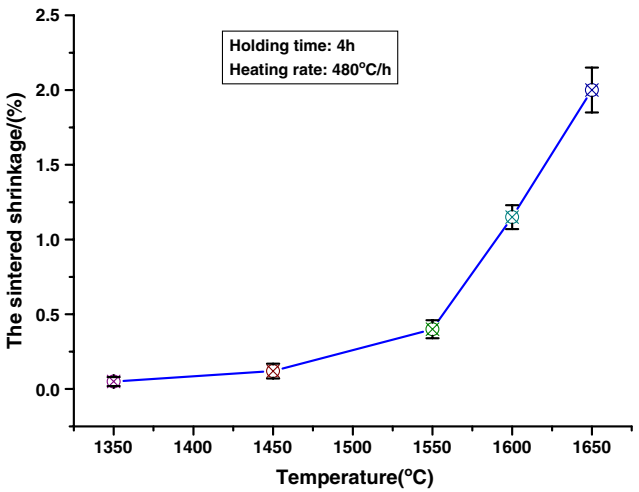

Fig. 7 The sintered shrinkage curve at different sintering temperatures

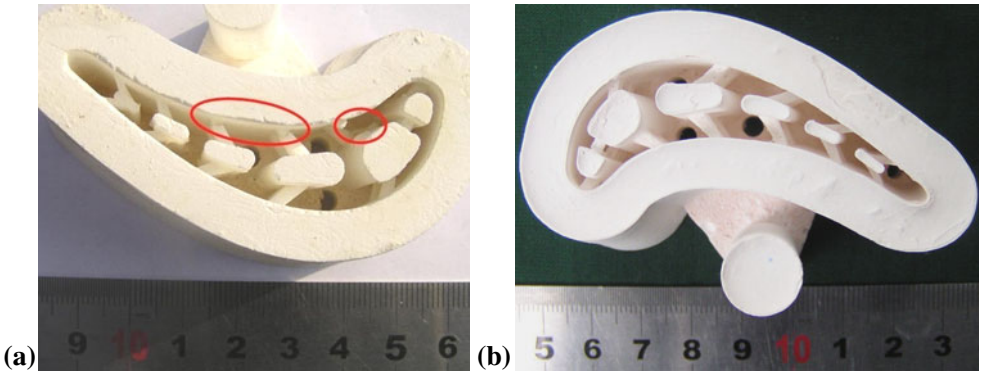

Fig. 8 **a** The SL mold prototype. **b** The integral ceramic mold

product of Al_2O_3 and MgO) may form at the range of 900–1,400°C, and yttrium aluminum garnet ($3Al_2O_3{\cdot}5Y_2O_3$, the reaction product of Al_2O_3 and Y_2O_3) is completed between 1,400 and 1,600°C [14, 15], and the sintering temperature of alumina power is usually higher than 1,500°C. Considering the sintered shrinkage and the sintering temperatures of alumina power, 1,550°C is chosen.

Figure 9 shows the sintered shrinkage curve of different holding times, as the sintering temperature is 1,550°C and the heating rate is 480°C/h. It can be seen that the sintered shrinkage is increased with holding time. The shorter holding time is favorable to obtain the lower shrinkage.

Figure 9 shows that the sintered shrinkage decreased with the increasing of the heating rate. When the heating rate increased from 240 to 540°C/h, the sintered shrinkage decreased from 1.12% to 0.28%, which meant that a higher heating rate was helpful to get a lower sintered shrinkage and maintain the structural integrality of the ceramic cores. A high heating rate could improve the efficiency, but excessive heating rate might lead to bulges on the surface of the green body (Fig. 10).

The sintered shrinkage could be reduced by decreasing the sintering temperature and holding time. In the paper, magnesium oxide powders were added to decrease the sintering temperature, which reacted with the finer corundum powders to form $MgAl_2O_4$, accompanied by a certain linear expansion (2.45%), which is helpful to compensate for the sintered shrinkage [15].

During the green body sintering process, excessive sintered shrinkage might lead to cracks and greater sintering stress in vulnerable areas of the ceramic mold. The proper sintering process parameters were determined as follows: the sintering temperature was 1,550°C, the heating rate was 360–540°C/h, and the holding time was 4 h.

Conventionally, once a job is received, hard tooling is designed and produced in order for the wax patterns and the ceramic cores to be injected. Depending on the complexity, these tools cost between ¥10,000 and ¥500,000, and take from 2 to 16 weeks to procure. In the novel process, the most obvious benefits were the savings resulting from the elimination of hard tooling. It took only 1 or 2 days to fabricate the SL mold and cost about ¥3000 (the SL mold weighs 300 g on average, and the price of DSM Somos19120 resin is ¥10 for each gram). Obviously, the new process presented in this paper costs less and performed higher efficiency in single piece or small batch production.

Compared with conventional investment casting for turbine blades, the characteristics of the new process are as follows:

(a) It is capable of producing turbine blades with abnormal film cooling holes, which cannot be manufactured by

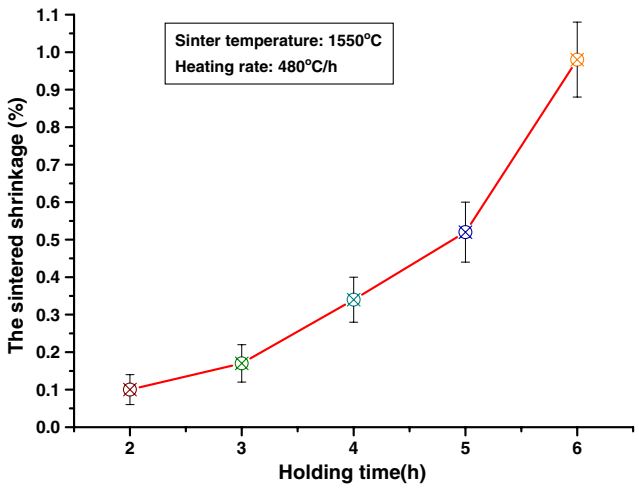

Fig. 9 The sintered shrinkage curve at different holding times

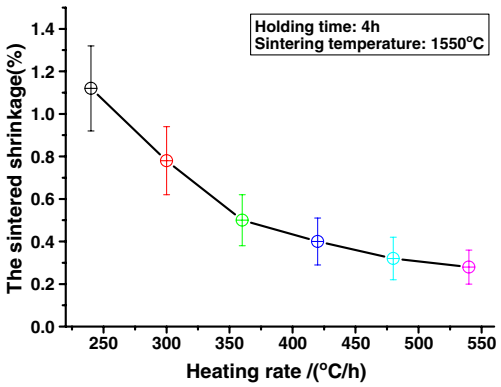

Fig. 10 The sintered shrinkage curve at different heating rates

conventional manufacturing methods; in addition, it is beneficial to guarantee the service performance and prolong the service life of turbine blade.

(b) There is no need to develop hard tooling; the production cost is remarkably reduced.

(c) It is quite suitable for new product development and single-piece or small-batch production; besides, the manufacturing cycle of the blade is only 2–3 weeks.

(d) The ceramic cores and shell are connected with each other during gelcasting, so there is no assembly tolerance any longer, and the ceramic cores do not deviate from original position during casting, which is helpful to improve casting yield.

4 Conclusions

A rapid prototype casting process was successfully developed by combining SL with gelcasting, which provided a sample and valid rapid prototyping to fabricate turbine blades with abnormal film cooling holes. The structural integrity of ceramic casting mold was maintained by adopting the freeze-drying process and the suitable sintering process. Compared with the conventional investment casting for turbine blades, the new process has a shorter process flow, a lower product cost, and a higher production yield. It is more suitable for new product development and single-piece or small-batch production.

Acknowledgements This research work was supported by "973 Program" of the People's Republic of China (Grant No. 2007CB707704) and Program for Changjiang Scholars and Innovative Research Team in University (IRT0646). The authors are grateful for the grants.

References

1. Gritsch M, Colban W, Schär H, Döbbeling K (2005) Effect of hole geometry on the thermal performance of fan-shaped film cooling holes. J Turbomach 127(4):718–725
2. Porter JS, Sargison JE, Walker GJ, Henderson AD (2008) A comparative investigation of round and fan-shaped cooling hole near flow fields. J Turbomach 130(4):1021–1028
3. Colban W, Thole KA, Haendler M (2008) A comparison of cylindrical and fan-shaped film-cooling holes on a vane endwall at low and high freestream turbulence levels. J Turbomach 130 (3):1007–1015
4. Wang XH, Fuh JYH, Wong YS, Tang YX (2003) Laser sintering of silica sand-mechanism and application to sand casting mould. Int J Adv Manuf Technol 21:1015–1020
5. Chua CK, Feng C, Lee CW, Ang GQ (2005) Rapid investment casting: direct and indirect approaches via model maker II. Int J Adv Manuf Technol 25(1–2):26–32
6. Lee CW, Chua CK, Cheah CM, Tan CH, Feng C (2004) Rapid investment casting: direct and indirect approaches via fused deposition modelling. Int J Adv Manuf Technol 23(1–2):93–101
7. Cheah CM, Chua CK, Lee CW, Feng C, Totong K (2005) Rapid prototyping and tooling techniques: a review of applications for rapid investment casting. Int J Adv Manuf Technol 25(3):308–320
8. Corcione CE, Greco A, Montagna F, Licciulli A, Maffezzoli A (2005) Silica moulds built by stereolithography. J Mater Sci 40 (18):4899–4904
9. Chockalingam K, Jawahar N, Ramanathan KN, Banerjee PS (2006) Optimization of stereolithography process parameters for part strength using design of experiments. Int J Adv Manuf Technol 29(1):79–88
10. Dickens PM, Stangroom R, Greul M, Holmer B, Hon KKB, Hovtun R, Neumann R, Noeken S, Wimpenny D (1995) Conversion of RP models to investment castings. Rapid Prototyping J 1(4):4–11
11. Yao WL, Leu MC (1999) Analysis of shell cracking in investment casting with laser stereolithography patterns. Rapid Prototyping J 5(1):9–12
12. Dotchev K, Soe S (2006) Rapid manufacturing of patterns for investment casting: improvement of quality and success rate. Rapid Prototyping J 12(3):156–164
13. Liu H-C, Lee S, Kang S, Edwards CF, Prinz FB (2004) RP of Si_3N_4 burner arrays via assembly mould SDM. Rapid Prototyping J 10(4):239–246
14. Medraj M, Hammond R, Parvez MA, Drew RAL, Thompson WT (2006) High temperature neutron diffraction study of the Al_2O_3–Y_2O_3 system. J Eur Ceram Soc 26:3515–3524
15. Mohapatra D, Sarkar D (2007) Preparation of MgO–$MgAl_2O_4$ composite for refractory application. J Mater Process Technol 189:279–283
16. Ma LG, Huang Y, Yang JL, Le HL, Sun Y (2005) Effect of plasticizer on the cracking of ceramic green bodies in gelcasting. J Mater Sci 40(18):4947–4949
17. Hague R, D'Costa G, Dickens PM (2001) Structural design and resin drainage characteristics of QuickCast 2.0. Rapid Prototyping J 7(2):66–72